Studies on surface composition and chemical states of calcium manganites

Sanjiv Kumar [a], V.S. Raju [a,*], Santanu Bera [b], K. Vijaynandhini [c], T.R.N. Kutty [c]

[a] *National Centre for Compositional Characterization of Materials, Bhabha Atomic Research Centre, ECIL Post, Hyderabad-500 062, India*
[b] *Water and Steam Chemistry Division, Bhabha Atomic Research Centre, Kalpakkam-440 024, India*
[c] *Materials Research Centre, Indian Institute of Science, Bangalore-560 012, India*

Abstract

This paper describes investigations on atomic composition and chemical states of sintered calcium manganites discs in surface and near surface regions. The atomic composition was determined by 3.05 MeV $^{16}O(\alpha,\alpha)^{16}O$ resonance elastic scattering while the chemical states by, X-ray photoelectron spectroscopy (XPS). The specimens examined included undoped and donor (Y^{3+}, Bi^{3+}) doped $CaMnO_3$, and Ca-excess and Mn-excess manganites namely Ca_2MnO_4 and $CaMn_2O_4$ respectively. Calcium manganite powder used in the preparation of discs was synthesized by a wet chemical method. X-ray diffraction (XRD) results indicated that all the discs are monophasic except $CaMn_2O_4$, which contained ~98% requisite manganite. The atomic compositions of undoped specimens are close to the stoichiometric value while Y^{3+} and Bi^{3+} doped specimens are deficient in Mn and O respectively. The O deficiency may be responsible for comparatively higher electrical conductivity of Bi^{3+} doped specimen. Some of the specimens were also examined subsequent to their annealing in low P_{O_2} atmosphere. This treatment produced significant compositional and structural modifications in the near surface regions. Mn(2p) electrons have identical binding energies in the sintered discs; therefore the valence states of Mn could not be discerned. However lesser binding energies of these electrons in annealed $CaMnO_3$ indicated the existence of Mn(II)/Mn(III) in the specimen.

Keywords: Calcium manganite; Backscattering spectrometry; X-ray photoelectron spectroscopy; Composition; Reduction

1. Introduction

Manganites with perovskite structure exhibit several interesting electronic and magnetic

* Corresponding author. Tel.: +91 40 27121365; fax: +91 40 27125463.
E-mail address: raju@cccmindia.org (V.S. Raju).

phenomena such as insulator-metal transition and colossal magnetoresistance (CMR) [1]. Consequently, these materials have been intensively studied in recent years [2,3]. These oxides can be represented by a general formula $Ln_{1-x}A_xMnO_3$ with Ln being a rare earth element and A, an alkaline earth element. The properties of materials depend on the content of x, nature and extent of doping and processing parameters. $CaMnO_3$, the basic unit of these perovskites, is itself of great interest. It is an n-type semiconducting oxide and exhibits anti ferromagnetic ordering at $T_N <$ 130 K as well. Incorporation of dopants introduces significant changes in the electrical properties of the material [4]. It can also be electron doped by annealing in lower P_{O_2} atmosphere to produce oxygen deficient nonstoichiometric perovskite, $CaMnO_{3-\delta}$ [5]. The electrical and magnetic properties of $CaMnO_{3-\delta}$ are influenced by oxygen content as well as the valence states of manganese [6].

Surface characterization of manganites is important in fabricating multilayer thin film devices that make use of the CMR properties. In the present work we have studied the atomic composition, in the near surface regions, of sintered discs of undoped and donor (3 at% Bi^{3+} and Y^{3+}) doped $CaMnO_3$ as well as Ca-excess and Mn-excess manganites namely Ca_2MnO_4 and $CaMn_2O_4$ respectively by 3.05 MeV $^{16}O(\alpha,\alpha)^{16}O$ elastic resonance scattering. Some of the specimens were also examined subsequent to their annealing in hydrogen atmosphere to study the compositional and structural variations accompanying the reduction process. This resonance scattering with significantly higher cross section is a well established backscattering spectrometry technique for depth profiling oxygen in the near surface regions non-destructively [7]. It has been used in the analysis of several oxide matrices including Y–Ba–Cu–O superconductors [8]. However such a study on manganites is lacking as most analytical studies deal with the determination of oxygen by classical chemical methods. The estimated composition has been discussed in correlation with structural and phase analysis of the ceramics by XRD. In addition, we have also investigated the chemical states of manganese in these oxides by XPS.

2. Experimental

2.1. Sample preparation

Polycrystalline samples of calcium manganite were synthesized by a wet chemical method involving a redox reaction between Mn(VII) and Mn(II) salts in nitric acid medium the details of which are reported in a previous publication [9]. Briefly concentrated HNO_3 was added to aqueous solution of $KMnO_4$ to maintain the pH in 1–2 range and heated to boiling conditions. The homogeneous solution of $Ca(NO_3)_2 \cdot 4H_2O$ and $MnSO_4 \cdot H_2O$, mixed in the desired ratio, was added to the boiling $KMnO_4$ solution to precipitate $MnO_2 \cdot xH_2O$. Due to its larger porosity and high surface area, the precipitated $MnO_2 \cdot xH_2O$ adsorbed other cations. The pH was raised to 7 by adding 2 M ammonium carbonate to complete the precipitation of the metal cations. The precipitate was filtered and washed with deionised water for complete removal of anions such as Cl^- and SO_4^{2-} and subsequently oven dried at 373 K. The dry powder was decomposed at 850 K followed by calcination at 1373 K for 5 h. The powder of calcium manganite thus obtained was mixed with 0.1 wt.% polyvinyl alcohol, a binder, and then pressed into pellets (thickness, 2 mm; diameter, 10 mm) in a hydraulic press at 200 MPa and subsequently sintered in air at 1573 K for 3 h. Specimens doped with 3 at% Bi^{3+} and Y^{3+} were prepared by intimately mixing the oxides of Y and Bi in the requisite proportions with calcium manganite powder and calcining at 1000 K for 3 h. The doped powder was then pelletised and sintered as described earlier. Some of the sintered specimens were annealed in $N_2 + H_2$ (1:1) atmosphere at 1373 K for 2 h to produce O deficient manganites.

2.2. Backscattering spectroscopy (BS) measurements

The BS measurements were carried out using 3 MV Tandetron at National Centre for Compositional Characterisation of Materials (NCCCM), Hyderabad. The α particle beam (ϕ = 1.5 mm) of requisite energy impinged on the targets at normal incidence in a typical scattering chamber. The

vacuum in scattering chamber, pumped by a turbomolecular pump, was about 2×10^{-6} Torr. An electron suppressor with -900 V was placed in front of the samples. The particles scattered at 170° were measured with a surface barrier detector and the data acquired on a PC based multichannel analyser.

2.3. Determination of atomic composition

The $^{16}O(\alpha,\alpha)^{16}O$ resonant scattering occurs at the surface when the target is bombarded with 3.05 MeV α particles. It occurs from deeper layers of the target at higher incident energies. Therefore the depth profiling of O is accomplished by increasing the incident beam energy beyond 3.05 MeV in steps.

The relative atomic composition of $CaMn_pO_q$ by this method can be estimated by using the formula:

$$q = R \times [\varepsilon(\mathrm{Ca}) + p\varepsilon(\mathrm{Mn})]/[\varepsilon(\mathrm{Si})/2 + (1-R) \times \varepsilon(\mathrm{O})] \quad (1)$$

where ε is the stopping cross section of the elements in the brackets, R is the ratio of resonant O yields for $CaMn_pO_q$ and a 3000 Å SiO_2 film, used as a standard for oxygen. The quantity p was determined from the BS spectrum by taking the signals of Ca and Mn into consideration. It is noted that their scattering cross sections are Rutherford in the beam energy region used in the experiments.The depth scale was established by the relation $(E_\alpha - E_r)/S(E)$ where E_α is the energy of the incident beam, E_r is the resonance energy and $S(E)$ is the stopping power at E_r. The stopping cross sections and powers were computed by SRIM 2000. The density of the discs required for computing $S(E)$ was estimated by geometrical methods.

2.4. XPS and XRD measurements

The XPS measurements were performed with VG-Scientific ESCALAB Mk200X machine, using Al Kα X-rays in a vacuum of 2×10^{-9} Torr. The energy scale of the spectrometer was calibrated with pure Ag and Cu samples. The binding energies were measured with a precision of ± 0.25 eV. The XRD measurements for identifying crystalline phases in the ceramics were carried out by a Scintag (USA) diffractometer with Cu Kα radiation.

3. Results and discussion

The specimens are well sintered to more than 95% of theoretical density. XRD results indicate the sintered discs of $CaMnO_3$, undoped as well as doped with 3 at% Y^{3+} and Bi^{3+}, are monophasic with perovskite structure and orthorhombic symmetry of space group Pbma. The disc of Ca_2MnO_4 is also phase singular having K_2NiF_4 type structure while that of $CaMn_2O_4$ contains ~98% of the desired manganite, with marokite structure together with the minor phase of $CaMnO_3$. The annealing of $CaMnO_3$ and $CaMn_2O_4$ in hydrogen atmosphere resulted in the formation of defect rock salt $CaMnO_2$, and $CaMnO_{2.5}$ of brownmillerite type structure, respectively. The different phases present in sintered and annealed specimens along with their crystal symmetries are given in Table 1.

Fig. 1(b)–(d) shows backscattered spectra from an undoped sintered $CaMnO_3$ specimen recorded with 3.07, 3.13 and 3.23 MeV α particles for depth profile measurements of oxygen. The occurrence of oxygen signal as a strong peak is due to $^{16}O(\alpha,\alpha)^{16}O$ resonant scattering. This approach is clearly advantageous over conventional RBS where the oxygen signal, as shown in Fig. 1(a), appears a weak step over the signals of Ca and Mn. The oxygen signal in Fig. 1(b)–(d) is a measure of its content at a depth of about 600 Å, 2500 Å and 5300 Å respectively. The height of oxygen signal decreases while its width increases with beam energy due to straggling effects but the area under the signal is constant for a homogeneous target.

Fig. 2(a) is the backscattered spectrum for an undoped sintered $CaMnO_3$ while Fig. 2(b) is from the same specimen annealed in hydrogen atmosphere. These spectra are normalized with respect to charge. It can be readily seen that in comparison to the sintered specimen, the annealed specimen has two significantly different spectral features: (1) the oxygen signal intensity is diminished and

Table 1
Phases, crystal symmetries and resistivities of calcium manganites at 293 K

Composition	Phase contents	Crystal symmetry	Resistivity (Ω cm)
$CaMnO_3$	Perovskite	Orthorhombic	0.84
$CaMnO_3$ (3 at% Y^{3+})	Perovskite	Orthorhombic	0.12
$CaMnO_3$ (3 at% Bi^{3+})	Perovskite	Orthorhombic	0.06
Ca_2MnO_4	K_2NiF_4 type structure	Tetragonal	–
$CaMn_2O_4$	98.5% Marokite 1.5% Perovskite	Orthorhombic Cubic	8×10^3
$CaMnO_3$[a]	Rock salt ($CaMnO_2$)	Cubic	–
$CaMn_2O_4$[b]	Brownmillerite ($CaMnO_{2.5}$)	Cubic	–
$CaMn_2O_4$[c]	88% Marokite 12% Perovskite	Orthorhombic Cubic	–

(–): Not measured.
[a] $CaMnO_3$ annealed in $N_2 + H_2$ (1:1) atmosphere at 1373 K for 3 h.
[b] $CaMn_2O_4$ annealed in $N_2 + H_2$ (1:1) atmosphere at 1373 K for 3 h (top portion).
[c] $CaMn_2O_4$ annealed in $N_2 + H_2$ (1:1) atmosphere at 1373 K for 3 h (cleaved portion).

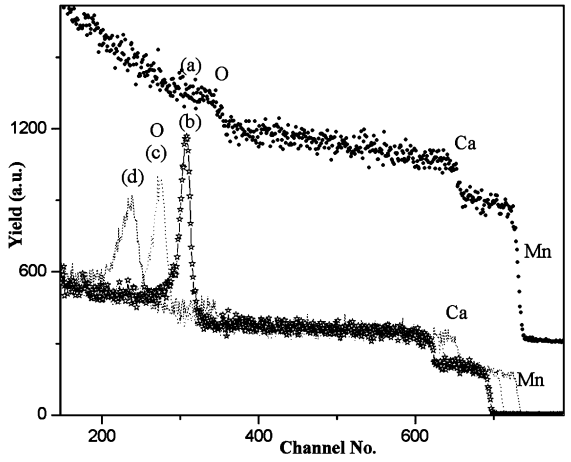

Fig. 1. (a) 2.4 MeV α-RBS spectrum form $CaMnO_3$ and (b), (c) and (d) depth profile of oxygen in $CaMnO_3$ obtained with 3.07, 3.13 and 3.23 MeV α particles respectively.

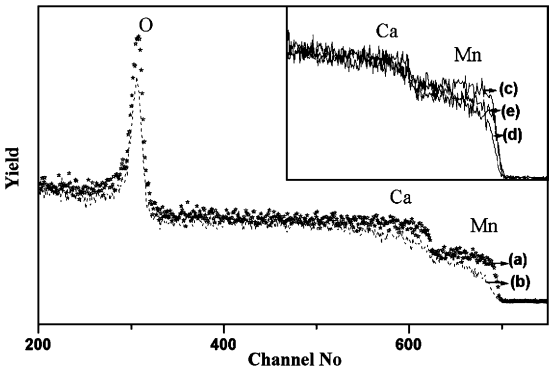

Fig. 2. 3.07 MeV α-backscattered spectra from (a) sintered $CaMnO_3$ and (b) after annealing it in hydrogen atmosphere. Inset shows the leading edges of Mn and Ca from (c) sintered $CaMn_2O_4$ (d) after annealing in hydrogen and (e) cracked interior surface of the annealed specimen.

(2) the slopes of the leading edges of cations, Mn in particular, are less. These features are indicative of surface modifications resulting from annealing with the decrease in oxygen signal intensity signifying, expectedly, the reduction of the specimen. The second feature showing the depletion of Ca and Mn in the near surface regions is, however, interesting. The reduced specimen of $CaMn_2O_4$ also exhibits similar spectral features. The 3.07 MeV α backscattered spectra from this manganite and its annealed form are shown in Fig. 2(c) and (d) respectively for illustration. The specimen had in fact cracked horizontally into two parts during annealing. The spectrum in Fig. 2(d) is from the top part of the cracked sample. The underlying part was also examined along the surface exposed due to cracking and the resulting spectrum is shown in Fig. 2(e). It is observed by comparing the spectra in Fig. 2(c)–(e) that the slopes of the leading edges of Ca and Mn for the bottom part are more than those of the corresponding top part of annealed disc but still less than the sintered specimen. This can be attributed to the mild reduction of the specimen with crack facilitating the process. It is supported by the fact that the bottom part contains marokite as the major phase (88%) while the top part as mentioned earlier, contains

only brownmillerite phase. It suggests that the interiors of the samples were not affected by annealing.

The atomic composition of different specimens as a function of depth determined by 3.05 MeV $^{16}O(\alpha,\alpha)^{16}O$ resonant scattering is listed in Table 1. The errors in the estimation of atomic ratio of Ca to Mn and depth profiles of oxygen are about 3% and 6% respectively. These are however higher in the case of reduced specimens due to rapidly varying signal intensities. The estimated compositions of the undoped $CaMnO_3$ and Ca_2MnO_4 are in agreement with their respective nominal stoichiometries. The Y^{3+} doped $CaMnO_3$ specimen is deficient in Mn while the one doped with Bi^{3+}, in oxygen. It is to be noted that the oxygen content in the Bi^{3+} doped specimen is marginally less that the error associated with its measurement. Nevertheless in view of the constancy of the value for repeated measurements, one at even higher depth, it can be surmised that the specimen is depleted in oxygen in comparison to undoped or Y^{3+} doped $CaMnO_3$. $CaMn_2O_4$ is enriched with Mn while oxygen stabilizes to its stoichiometric value at a depth of about 2000 Å. The excess of oxygen in surface regions may be due to adsorbed oxygen bearing species. In the case of annealed specimens, it is evident that reduction in hydrogen atmosphere causes considerable alteration in the composition with the relative contents of Mn and O decreasing significantly, particularly in the case of $CaMn_2O_4$. Further, the atomic composition of the bottom portion of the cracked specimen of $CaMn_2O_4$ is nearly identical to that of sintered $CaMn_2O_4$ due to its reduction to a lesser extent. It is in agreement with the conclusions drawn from the qualitative spectral analysis.

The reduction of $CaMnO_3$ and $CaMn_2O_4$ to $CaMnO_2$ and $CaMnO_{2.5}$ respectively involves loss of oxygen according to the following reactions:

$$CaMn^{+4}O_3 \rightarrow CaMn^{+3}O_{2.5} \rightarrow CaMn^{+2}O_2$$

$$CaMn_2O_4 \rightarrow CaMn^{+4}O_3 \rightarrow CaMn^{+3}O_{2.5}$$

The phase singularity of annealed $CaMnO_3$ is in agreement with the above formalism. However, the conformity observed between the compositional and phase analyses of sintered specimens is lacking, as there is a significant gradient in the concentration of oxygen in the surface regions. Furthermore, the depletion of Ca and Mn in identical concentrations maintains the relative atomic ratio of Ca and Mn close to unity. The surface depletion of Mn on reduction is distinctly observed in the case of $CaMn_2O_4$. So far as its reduction formalism is concerned, the formation of $CaMnO_3$ in the first step of the reaction is confirmed by increase in the content of $CaMnO_3$ phase from 1.5% in the sintered $CaMn_2O_4$ to 12% in the mildly reduced bottom portion of the cracked specimen. Calcium manganites thus formed are obviously accompanied by manganese oxides that are often non-stoichiometric. It is to be noted that depletion of Mn does not imply its loss, as manganese oxides are nonvolatile even at higher temperatures. Under this consideration, the present observation can be ascribed to either precipitation and or migration of Mn bearing species during the reduction process, which escape detection, by XRD and BS. The non-stoichometric phases formed often lack sufficiently large crystalline domains and therefore may not be identified by conventional structure determination technique.

The specimens were analysed by core level XPS to obtain information on the chemical states of the constituents. Fig. 3 shows the Mn(2p) electron spectra of different specimens. The spectra exhibit

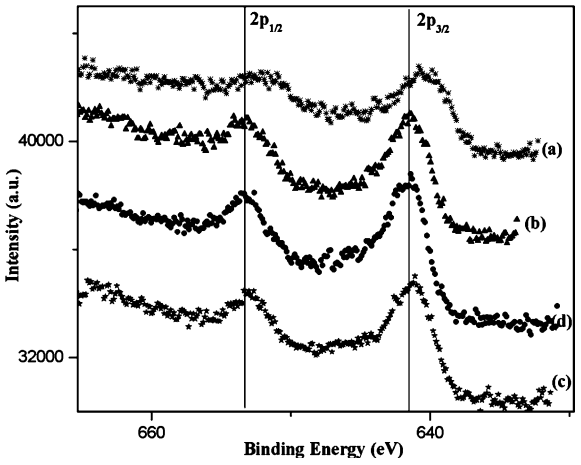

Fig. 3. Mn(2p) electron spectra of (a) $CaMnO_3$ (reduced), (b) $CaMn_2O_4$ (sintered), (c) $CaMn_2O_4$ (reduced, top portion) and (d) $CaMn_2O_4$ (reduced, cracked portion).

$2p_{1/2}$ and $2p_{3/2}$ spin–orbit doublets. The Mn(2p) peaks, in agreement with previous studies, are broad and asymmetrical towards high binding energy side [10]. Abbate et al. have explained the reasons for the larger breadth of the peaks [11].

Oku et al. have measured the binding energies of $Mn(2p_{3/2})$ electrons in different manganese oxides [12]. These are also listed in Table 2. It can be seen that the chemical shift is appreciable only in MnO and MnO_2. The study also concluded neither the two oxidation states of Mn in Mn_3O_4 nor Mn site differences in Mn_2O_3 are distinguishable by XPS. In previous XPS studies on $CaMnO_3$ and several $CaMnO_{3-\delta}$ compounds with different δ values, the binding energy of Mn $2p_{3/2}$ electrons was reported to be identical (641.9 eV) in each compound [13]. However in the present studies, it is about 641.7 eV in all the specimens except annealed $CaMnO_3$ where it is about 640.6 eV. It is to be noted that the surfaces of reduced specimens were distinctly green providing indication of existence of Mn in +3 valence states. The higher binding energy of Mn $2p_{3/2}$ electrons in air sintered $CaMnO_3$ suggests Mn to be in +4 valence state, occupying sites with octahedral O coordination. The reduction of $CaMnO_3$ involves introduction of O vacancies and conversion of Mn^{4+} ions into lower oxidation states. The lower binding energy in $CaMnO_{3-\delta}$ is indicative of this process. The differences in the binding energies in $CaMnO_{3-\delta}$ in the present study and [13] may be due to different conditions of reduction. MnO and CaO also have rocksalt structure. The lower binding energies of Mn (2p) electrons in such samples eliminate the possibility of formation of MnO, which due to its pyrophoric nature, gets converted to Mn_3O_4. Similarly CaO reacts with atmospheric CO_2, to produce $CaCO_3$. The C (1s) electron spectra of each specimen showed only one peak corresponding to the adventitious carbon. The absence of a peak in 287–289 eV in the C (1s) spectra, characteristic of CO_3^{2-}, is therefore indicative of the absence of CaO as well. The binding energies of Ca(2p) electrons in the specimens are also nearly identical. The slight variation in their values is due to different crystal structures of the specimens (Table 3).

Table 2
Atomic composition of calcium manganite specimens in near surface regions

Sample	Depth (Å)	Atomic composition (N_{Ca}:N_{Mn}:N_O)
$CaMnO_3$	600	1.0:1.0:3.1
	2500	1.0:1.0:3.1
$CaMnO_3$[a]	600	1.0:0.9:1.5
	1700	1.0:0.9:2.2
	2500	1.0:0.8:2.4
$CaMnO_3$ (3 at% Y^{3+} doped)	600	1.0:0.9:3.2
	2500	1.0:0.9:3.1
$CaMnO_3$ (3 at% Bi^{3+} doped)	600	1.0:1.0:2.8
	2500	1.0:1.0:2.8
	5100	1.0:1.0:2.8
$CaMn_2O_4$	800	1.0:2.2:4.4
	2800	1.0:2.2:4.1
	3800	1.0:2.2:4.2
$CaMn_2O_4$[b]	800	1.0:1.2:2.0
	2800	1.0:1.2:1.9
	3800	1.0:1.1:1.6
$CaMn_2O_4$[c]	800	1.0:2.0:3.8
	1900	1.0:2.1:3.9
	3800	1.0:2.0:4.1

[a] $CaMnO_3$ annealed in $N_2 + H_2$ (1:1) atmosphere at 1373 K for 3 h.
[b] $CaMn_2O_4$ annealed in $N_2 + H_2$ (1:1) atmosphere at 1373 K for 3 h (top portion).
[c] $CaMn_2O_4$ annealed in $N_2 + H_2$ (1:1) atmosphere at 1373 K for 3 h (cracked bottom portion).

Table 3
Binding energies (eV) of Mn 2p and Ca 2p electrons in calcium manganites

Sample	Mn		Ca	
	$2p_{3/2}$	$2p_{1/2}$	$2p_{3/2}$	$2p_{1/2}$
$CaMnO_3$	641.9	653.5	347.5	351.1
$CaMnO_3$[a]	640.8	652.2	347.3	351.0
$CaMn_2O_4$	641.8	653.4	347.5	351.0
$CaMn_2O_4$[b]	641.4	653.0	347.3	351.0
$CaMn_2O_4$[c]	641.7	653.3	347.4	351.1
MnO	640.6	652.2	–	–
Mn_3O_4	641.4	653.0	–	–
Mn_2O_3	641.9	653.5	–	–
MnO_2	642.2	653.8	–	–

[a] $CaMnO_3$ annealed in $N_2 + H_2$ (1:1) atmosphere at 1373 K for 3 h.
[b] $CaMn_2O_4$ annealed in $N_2 + H_2$ (1:1) atmosphere at 1373 K for 3 h (top portion).
[c] $CaMn_2O_4$ annealed in $N_2 + H_2$ (1:1) atmosphere at 1373 K for 3 h (cracked bottom portion).

Fig. 4 shows the temperature dependence of electrical resistivity, ρ versus T, for undoped and doped $CaMnO_3$. It is evident that doping with either Y^{3+} or Bi^{3+} causes a decrease in the resistivity of $CaMnO_3$. The doped specimens exhibit metal to insulator transition at around 160 K. The resistivity of manganites depends on several factors including the valence states of Mn and oxygen non-stoichiometry. Double exchange mechanism which involves hopping of electrons from Mn^{3+} ($t_{2g}^3 e_g$) onto Mn^{4+} (t_{2g}^3) is usually invoked to explain variations in resistivity [6]. The doping of $CaMnO_3$ at Ca sites with trivalent Y^{3+} or Bi^{3+} ions introduces electrons by way of charge compensation leading to the formation Mn^{3+} in the matrix such that it is represented as $Ca_{1-x}Y(Bi)_xMn^{4+}_{1-x}\,Mn^{3+}_xO_3$. Therefore the resistivities of the doped materials are less. Further, it is observed that the resistivity of Bi^{3+} doped specimen is the lowest, which can be attributed to its oxygen deficiency. The removal of one oxygen ion (O^{2-}) results in the generation of two Mn^{3+} ions causing an increase in Mn(III) concentration and hence the increased conductivity of the material. However we could not explain the effect of Mn deficiency in the Y^{3+} doped specimen. The present study shows that dopants of similar charges may not introduce identical compositional changes. Resistivity measurements could not be performed on reduced specimens in view of the presence of micro cracks. However previous reports suggest that the resistivity of reduced manganites, $CaMnO_{3-\delta}$ is strongly influenced by oxygen deficiency, which controls the concentration of Mn^{3+} ions and, in turn the resistivity [6].

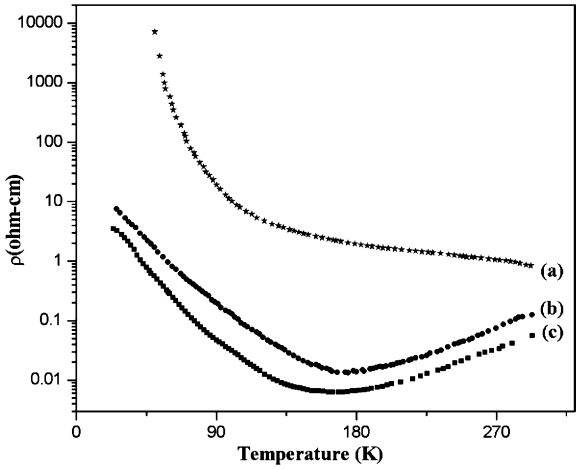

Fig. 4. Resistivity versus temperature plot for (a) undoped, 3 at% Y^{3+} and (c) 3 at% Bi^{3+} doped $CaMnO_3$.

4. Summary

3.05 MeV $^{16}O(\alpha,\alpha)^{16}O$ resonant scattering with enhanced sensitivity for oxygen provides the compositional analysis of calcium manganites with reasonably good accuracy. Doping in the Mn site of $CaMnO_3$ with donors such as Y^{3+} or Bi^{3+} causes compositional changes in the material, which affect its electrical characteristics. However the phase identity of $CaMnO_3$ (perovskite) is maintained on doping. Annealing of manganites in hydrogen atmosphere introduces significant structural and compositional changes that modify the modify the BS spectral features of the parent manganites. XPS measurements suggest the existence of Mn(II)/Mn(III) in the annealed specimens.

Acknowledgement

The first two authors thank Dr. J. Arunachalam, Head, NCCCM for useful discussions during the work.

References

[1] K. Chahara, T. Ohno, M. Kasai, S. Ikeda, Appl. Phys. Letts. 63 (1993) 1990.
[2] R. Von Helmolt, J. Wecker, B. Holzapfel, L. Schultz, K. Samwer, Phys. Rev. Lett. 71 (1993) 2331.
[3] J.J. Neumerier, J.L. Cohn, Phys. Rev. B 61 (2000) 14319.
[4] B. Raveau, Y.M. Zhao, C. Martin, M. Hervieu, A. Maignan, J. Solid State Chem. 149 (2000) 203.
[5] K.R. Poeppelmeirier, M.E. Leonowicz, J.M. Longo, J. Solid State Chem. 44 (1982) 89.
[6] J. Briatico, B. Alascio, R. Allub, A. Butera, A. Caneiro, M.T. Causa, M. Tovar, Phys. Rev. 53 (1996) 14020.
[7] J.A. Leavitt, L.C. McIntyre Jr., M.D. Ashbaugh, J.G. Oder, Z. Lin, B. Dezfouly-Arjomandy, Nucl. Instr. and Meth. B 44 (1990) 260.

[8] F.L. Freire Jr., C.V. Barros Leite, B.K. Patnaik, G.B. Baptista, D. Nagule, R.K. Pandey, W. Kirk, J. Appl. Phys. 65 (1989) 400.
[9] John Philip, T.R.N. Kutty, Mater. Chem. Phys. 63 (2000) 218.
[10] M.E.M. Jorge, A.C.D.S. Santos, M.R. Nunes, Int. J. Ing. Mats. 3 (2001) 915.
[11] M. Abate, F.M.F. de Groot, J.C. Figgle, A. Fujimori, O. Strebel, F. Lopez, Phys. Rev. B 46 (1992) 4511.
[12] M. Oku, K. Hirokawa, S. Ikrda, J. Electron. Spectrosc. 7 (1975) 465.
[13] G. Zampieri, F. Prado, A. Canerio, J. Briatico, M.T. Causa, M. Tovar, B. Alasscio, M. Abbate, E. Morikawa, Phys. Rev. B 58 (1998) 3755.